Erschienen in: Polymer Chemistry ; 12 (2021), 21. - S. 3116-3123
https://dx.doi.org/10.1039/D1PY00394A

Compartmentalized polymerization in aqueous and organic media to low-entangled ultra high molecular weight polyethylene†

Florian P. Wimmer, Viktoria Ebel, Felix Schmidt and Stefan Mecking *

Catalytic copolymerization with functional group tolerant lipophilic Ni(II) catalysts in aqueous emulsion-type polymerization or dispersion polymerization in organic solvents (THF, *n*-heptane) yields ultra high molecular weight polyethylene (UHMWPE) as submicron- or micron-sized, respectively, particles. Precise multiblock copolymers with crystallizable C_{46} polyethylene blocks and amorphous soluble polybutene blocks, as well as a random ethylene-octene copolymer with similar block lengths were suitable for particle stabilization in the organic dispersion polymerizations.

Introduction

Ultra high molecular weight polyethylene (UHMWPE) provides an exceptional materials performance, and at the same time it is accessible in a resource efficient manner. Its synthesis by catalytic polymerization of ethylene compares favourably to more complex multi-step routes required to prepare other high performance materials.

The outstanding abrasion resistance of UHMWPE results from the extremely long chains, which can span several otherwise separate crystalline lamellae. However, they also result in a poor processability due to the high number of entanglements that usually occur in the melt.[1–3] This hampers a more widespread use of this otherwise desirable material. Therefore, reducing the number of entanglements in the nascent polymer as obtained from polymerization has been a long sought after goal to achieve melt-processable UHMWPE.[4] The key to formation of low entangled UHMWPE is a sufficiently rapid crystallization of the formed polymer chains relative to the chain growth rate, and keeping nascent crystallites separate during nucleation.[5] These prerequisites are typically achieved by polymerizing at high dilutions (usually around 1 wt% UHMWPE)[6,7] and at low temperatures which result in very rapid crystallization.[5]

An alternative approach is polymerization in compartmentalized systems. By polymerization in confined spaces, like droplets or small particles, any entanglements formed are confined to the given individual compartment, resulting in an overall low-entangled nascent polymer powder as a product. To this end Ronca *et al.* obtained 'colloidal UHMWPE' by polymerization in toluene solvent in the presence of LLDPE as a stabilizer. The latter co-crystallized with the nascent polyethylene creating a polymer corona on the UHMWPE crystallites, which provided steric stabilization.[8] Particles with sizes of several μm were obtained. As a different approach, compartmentalization can be promoted by polar reaction media. This requires catalysts compatible with such media, a realm of late transition metal complexes. To achieve high molecular weights and linearities, the general tendency of d^8 metal complexes for chain transfer and branch formation *via* β-hydride formation needs to be overcome. This has most recently been achieved by state of the art neutral Ni(II) catalysts, that form UHMWPE in THF solutions or aqueous systems.[9–11] In the latter case, with water-soluble catalyst precursors starting from a single homogeneous aqueous phase fully disentangled UHMWPE is obtained in the form of colloidally stable single chain single crystals.[12,13]

We now further elaborate the concept of colloidal UHMWPE synthesis to aqueous emulsion systems and lipophilic catalyst precursors as well as non-aqueous compartmented systems.

Results and discussion

Polymerization with aqueous mini-emulsions

Lipophilic catalyst precursors are synthetically more easily accessible and have been reported in broader variety than their hydrophilic counterparts. To be able to apply them, a miniemulsion protocol was employed. This protocol, previously established for the synthesis of HDPE and branched copolymers,[14–16] starts from an aqueous miniemulsion of a

Chair of Chemical Materials Science, Department of Chemistry, University of Konstanz, 78464 Konstanz, Germany. E-mail: stefan.mecking@uni-konstanz.de

solution of the catalyst precursor in a small volume of water-immiscible organic solvent.

Emulsification is achieved by subjecting a mixture of an aqueous surfactant solution with the catalyst solution to high shear, usually introduced by ultrasonication. In a typical polymerization experiment in this work, the lipophilic catalyst precursor was dissolved in a small volume of a non-water-miscible solvent (*e.g.* 2 mL of benzene, toluene, *m*-xylene or mesitylene). This lipophilic phase was dispersed in 100 mL of an aqueous surfactant solution (sodium lauryl sulfate) through ultrasonication. The resulting miniemulsion was transferred into a pressure autoclave and stirred under 40 bars of ethylene pressure. For this work, catalyst motif **1-L** (*cf.* Fig. 1) was employed which has been proven to afford UHMWPE with $M_n = 4 \times 10^6$ g mol^{-1} in the aforementioned polymerization in aqueous solution to single crystals.[13]

As anticipated, under otherwise identical conditions (30 °C) polymerization with the miniemulsion system with **1-py** yields much larger particles compared to the aqueous soluble **1-H$_2$N-PEG** reference (Table 1, entry 1 *vs.* 4). Polymer molecular weights are comparable in both cases. Compared to ideal conditions (15 °C) for the reference system (entry 3), molecular weights are lower due to enhanced chain transfer with increasing polymerization temperature. The activity of the miniemulsion system with **1-py** is considerably lower (entries 1 *vs.* 4. Note that **1-py** did not yield any significant amount of polymer at 15 °C under otherwise identical conditions as entry 1). This can be due to an incomplete dissociation of pyridine from the catalyst precursor, and competition of monomer coordination with pyridine coordination during polymerization that results in dormant species. By contrast, in the reference system dissociation of the labile hydrophilic NH_2-PEG ligand is enhanced by the formation of the new polymer nanoparticle phase.[17] Accordingly, productivity with **1-py** is increased at 60 °C, but still lower than for the reference and at the expense of molecular weight (entry 2). To address this issue, more weakly coordinated catalyst precursors that can also be generated in a straightforward *in situ* protocol were studied. Dissolution of the corresponding salicylaldimine ligand in an appropriate solvent and addition of 1.1 eq. of [(tmeda)NiMe$_2$] as Ni(II) precursor[18] resulted in the immediate formation of the desired nickel complex as evidenced by a new Ni-*Me* ^{1}H NMR resonance at −1.29 ppm and complete disappearance of the resonance at −0.45 ppm (Fig. 2). Subsequent mixing with 100 mL of aqueous surfactant solution and emulsification by ultrasonication resulted in clear to slightly opaque miniemulsions with an orange color originating from the salicylaldiminato Ni(II)-Me catalyst precursor. Note that in the case of low catalyst loadings (*i.e.* 10 μmol and below), a slightly higher excess of 1.5 equivalents of [(tmeda)NiMe$_2$] proved beneficial for the productivity of polymerizations, likely due to a partial consumption of this reactive nickel compound by impurities present in the reaction mixture.

Exposure of these catalyst miniemulsions to ethylene in a pressure reactor resulted in the formation of colloidally stable dispersions of UHMWPE with M_n up to 2×10^6 g mol^{-1} (Table 2). As expected for a heterophase polymerization with the additional feature of continuous mass transfer of monomer from the gas phase to the aqueous liquid phase, the outcome of polymerization depends strongly on the efficiency of mixing. Efficient polymerization productivities required stirring rates of 500 rpm or higher at the catalyst loadings employed. Stirring at a high rate of 1000 rpm resulted in loss

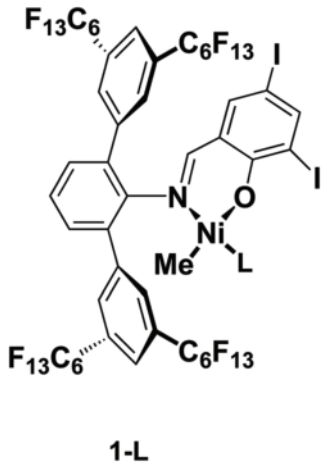

1-L

Fig. 1 Catalyst precursor employed in aqueous miniemulsion (L = pyridine, py), and water-soluble reference system (L = NH_2-PEG).

Table 1 Polymerization in aqueous media with pyridine-coordinated catalyst precursors and water-soluble reference catalysts

Entry	*t* reaction [°C]	Labile ligand L	Yield [g]	Activity[a]	Chains/ [Ni]	T_m[b] [°C]	χ[b] [%]	M_n[c] [×10^3 g mol^{-1}]	M_w/M_n[c]	Particle size[d] [nm]	Particle PDI[d]
1	30	Pyridine	1.0	1.8	0.6	140 (137)	73 (52)	220	1.4	228	0.20
2	60	Pyridine	2.3	4.1	3.3	128 (127)	41 (47)	90	1.5	217	0.19
3	15	NH_2-PEG	5.0	12	0.6	140 (136)	71 (47)	840	1.08	22	0.18
4	30	NH_2-PEG	5.9	14	1.7	134 (133)	54 (46)	340	1.9	21	0.07

Polymerization conditions: entries 1 and 2: 7.5 μmol precatalyst, 2 mL toluene. Entries 3 and 4 10 μmol precatalyst, 2 mL hexafluorobenzene. General polymerization conditions: 120 min 40 bar ethylene, 100 mL water, 1000 rpm, 3 g SDS, 550 mg CsOH. Reaction mixtures were emulsified by 2 min of ultrasonication, transferred to the autoclave and pressurized. [a] Average activity, in units of 10^3 mol_E mol_{Ni}^{-1} h^{-1}. [b] Determined by DSC at a heating/cooling rate of 10 K min^{-1}. Data is reported from first heating cycles. Data from second heating cycles is given in brackets. [c] Molecular weights are determined by gel permeation chromatography in *o*-DCB at 160 °C *via* universal calibration with polystyrene standards. [d] Volume average particle sizes and polydispersity index as a measure of particle size distribution determined by DLS.

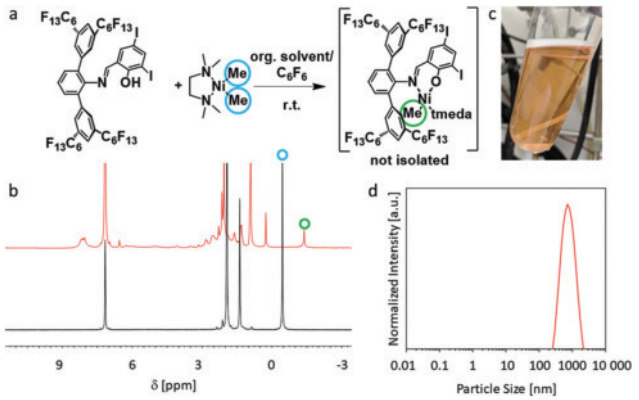

Fig. 2 (a) Reaction scheme of *in situ* generation of Ni(II) catalyst. (b) ^{1}H NMR spectra (400 MHz, 300 K, C_6D_6, 1 vol% C_6F_6) of [(tmeda)$NiMe_2$] (black) and immediately after addition of 0.9 eq. of the corresponding salicylaldimine (red). Ni-Me groups are assigned (colour coded) as indicated in a. (c) Representative image of miniemulsified catalyst solution. (d) DLS trace of polymer dispersion obtained after polymerization.

of colloidal stability and creaming of the formed polymer, likely due to shear-induced aggregation of the formed polymer particles.

These satisfactory results encouraged a screening of different hydrocarbon solvents for the catalyst in the miniemulsion procedure (Fig. 3). The nature of the solvent is expected to have a subtle but relevant impact on the emulsification process and the nature of the miniemulsion formed as well as on the early stages of polymerization in which phase separation of the forming polymer from the solvent and nucleation of particles occurs. Due to the high fluorine content of the salicylaldimine applied, its solubility is limited in most solvents. Small amounts (typically 10 vol%, depending on lipophilic solvent) of co-solvents such as hexafluorobenzene or THF enabled dissolution of all catalyst components in sufficient concentrations.

Even though heptane was found advantageous in terms of salicylaldimine solubility (no co-solvent required), polymerization did not yield colloidally stable polymer dispersions. By contrast, with different aromatic solvents stable dispersions were obtained. In terms of polymer molecular weight, *m*-xylene was found to be most suitable, also maintaining high polymerization activities at the same time. Note that the nominal values of chains per nickel are low, however, which suggests that only a part of the added catalyst precursor has been converted to active species in these experiments. The comparatively broad molecular weight distributions observed at lower stirring rates (Table 2) are likely due to a heterogeneous nature of the conditions (monomer concentration, colloidal state) experienced by the actives sites. At the polymerization temperature of 15 °C, intrinsic chain transfer is low as reflected by the possibility of living polymerization at this temperature (*cf.* Table 1).

Particle morphologies

UHMWPE particles obtained with the aqueous catalyst miniemulsions exhibit a multi-lamellae structure consisting of

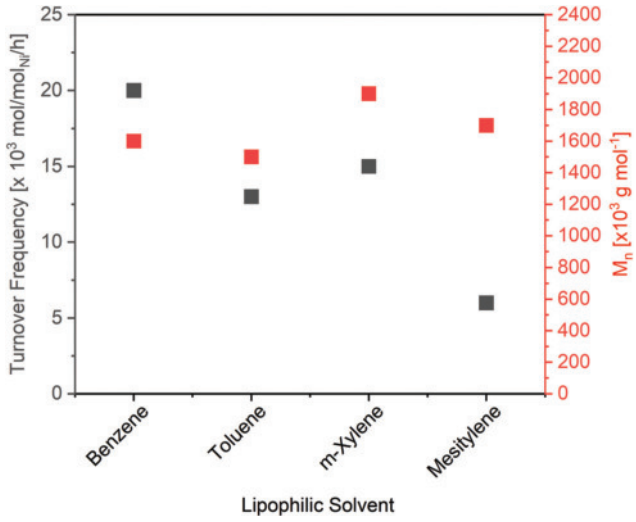

Fig. 3 Catalytic activity and polymer molecular weight observed with different aromatic solvents as the catalyst droplet phase in aqueous miniemulsion. For details *cf.* ESI.†

Table 2 Influence of stirring rate on the polymerization reaction in aqueous emulsion

Entry	Stirring rate [rpm]	Yield [g]	Activity[a]	Chains/ [Ni]	T_m[b] [°C]	χ[b] [%]	M_n[c] [$\times10^6$ g mol^{-1}]	M_w/M_n[c]	Particle size[d] [nm]	Particle PDI[d]
1	100	1.4	5.0	0.3	135 (133)	71 (54)	0.3	2.4	238	0.127
2	250	1.7	6.1	0.3	136 (133)	69 (52)	0.3	3.0	234	0.146
3	500	7.1	25	0.3	140 (134)	70 (45)	1.3	2.4	387	0.183
4	750	8.5	61	0.2	141 (135)	70 (45)	2.1	2.3	402	0.164
5	1000	3.9	14	0.2	142 (135)	69 (43)	1.3	1.5	—	—

Polymerization conditions: 20 μmol precatalyst (*in situ* generated from 22 μmol [(tmeda)$NiMe_2$], 20 μmol salicylaldimine ligand), 1.5 mL benzene + 0.5 mL hexafluorobenzene, 30 min, 40 bar ethylene, 15 °C, 100 mL water, 5 g SDS, 550 mg CsOH. Reaction mixtures were emulsified by 2 min of ultrasonication, transferred to the autoclave and pressurized. [a] Average activity, in units of 10^3 mol_E mol_{Ni}^{-1} h^{-1}. [b] Peak melting points and crystallinities were determined by DSC at a heating/cooling rate of 10 K min^{-1}. Data is reported from first heating cycles. Data from second heating cycles is given in brackets. [c] Molecular weights are determined by gel permeation chromatography in *o*-DCB at 160 °C *via* universal calibration with polystyrene standards. [d] Volume average particle sizes and polydispersity index as a measure of particle size distribution determined by DLS.

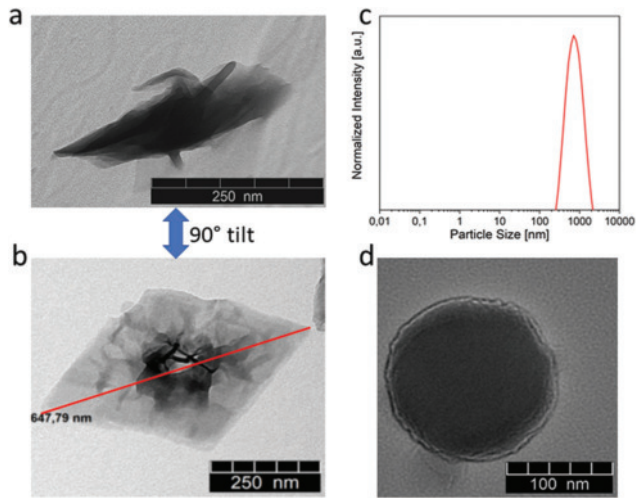

Fig. 4 (a/b) TEM micrograph and (c) DLS trace of UHMWPE particles obtained from aqueous polymerization at 15 °C (M_n = 1.7 × 10^6 g mol^{-1}, Table S3,† entry 4). (d) TEM micrograph of spherical UHMWPE particle after melting in dispersion.

several lozenge-shaped platelets of several hundred nanometers in size (Fig. 4). Particle sizes (from DLS) increase with increasing polymer yields (see Table 2) without an evident change in particle morphology (TEM) (see ESI†). Due to their comparably large size, the lamellae show a strong warping at the centre of the lozenges as reported for large lozenge-shaped single lamella polyethylene particles by Godin *et al.*[19] Tilting of the samples in the electron microscope further underlined the lamellae structure of the particles (Fig. 4a vs. b). Heating a diluted polymer dispersion above T_m to 160 °C for 1 h in a pressure-tight glass vial followed by rapid cooling to room temperature resulted in a change of particle shape from stacks of lozenge shaped lamellae to exclusively spherical particles with a smaller diameter and without evident lamellae. The compact spherical shape of these recrystallized particles enables a calculation of the number of chains per particle. A particle is composed of *ca.* 10^3 chains, based on $d_{particles}$(DLS) = 174 nm and M_n = 1.7 × 10^6 g mol^{-1}. Further, this experiment confirms that the crystalline morphology of the as-obtained particles is determined by the aqueous polymerization process.

Differential scanning calorimetry (DSC) was employed to estimate the degree of entanglements in UHMWPE samples. From studies of the melting kinetics of nascent-, melt-crystallized- and solution-crystallized UHMWPE samples with varying degrees of entanglements, Rastogi and co-workers[7,20] deduced that samples with a low degree of entanglement (either 'disentangled' nascent polymers or post-polymerization solution-crystallized polymers) feature a characteristic dependence of the observed melting point on the heating rate. This is attributed to detachment of the polymer chain from the polyethylene's crystal surface which is not possible in case of entangled samples (entangled nascent polymers or melt-crystallized polymers) due to constraints in the amorphous phase. The increased melting temperature of entangled polymer samples is caused by a higher activation energy of cooperative detachment of polymer chains from the crystal stem due to entanglements and tie-molecules.[20,21] This results in melting transitions of *e.g.* 141 °C and 135 °C (rapid heating, first and second heating cycle, respectively) and 135 °C in the first heating cycle at an ideal slow heating.

DSC traces (Fig. 5) of UHMWPE samples obtained with catalyst miniemulsions revealed a disentangled nature as concluded from the significantly lower peak melting temperature observed at a slower heating (1 K min^{-1}) *vs.* the standard heating rate of 10 K min^{-1}. By comparison, for a reference sample obtained by suspension polymerization in toluene under otherwise identical conditions (catalyst precursor **1-py**, 60 °C, 40 atm, M_n = 1.3 × 10^6 g mol^{-1}) indeed an entangled nature is suggested by DSC. All polymer samples obtained from aqueous emulsion polymerization in this work were found to be disentangled by this method.

Even though DSC suggests a low level of entanglements overall, we reasonably assume that within the multilamellar particles entanglements are formed between the proximate crystallites during the particle formation process. This would be welcome, as a certain low degree of entanglements is crucial to prevent fracturing along the crystal boundaries in solid state drawing steps during polymer processing.[22]

Polymerization in non-aqueous media

Polymerization in non-aqueous media can be complimentary to aqueous systems in terms of further processing of the material, compatibility with existing processes, and the scope of catalysts applicable. The concept of compartmentalization can be facilitated by non-aqueous media which are poor solvents for UHMWPE such as *n*-heptane or THF in combination with appropriate colloidal stabilizers. In such non-aqueous systems, steric stabilization is the method of choice. Their different segments provide an affinity with either phase. To

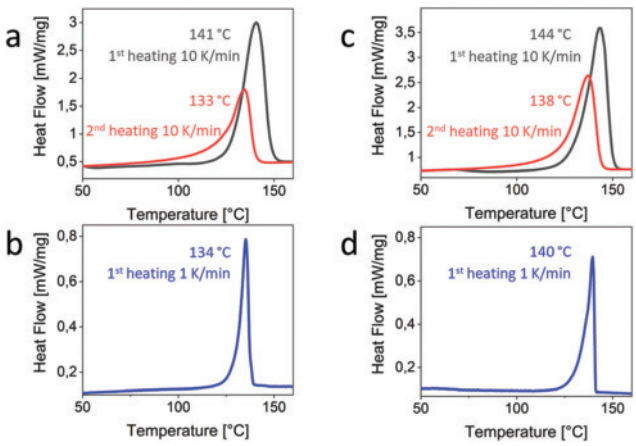

Fig. 5 DSC traces of UHMWPE obtained from aqueous miniemulsion polymerization (a) heating rate 10 K Min^{-1}, (b) 1 K min^{-1}. DSC traces of reference UHMWPE obtained from precipitation polymerization in toluene (c) 10 K min^{-1}, (d) 1 K min^{-1}.

this end, we studied well-defined multiblock copolymers with precise length linear sequences that can interact with the UHMWPE (by epitaxial crystallization or co-crystallization) and precise length branched blocks that enhance compatibility with the reaction medium (Fig. 6). These stabilizers were generated by polycondensation of dimethyl-1,48-octatetracontanedioate (from catalytic chain doubling of fatty acids[23]) with hydrogenated 1,2-polybutadienediol (PBDD)[24] in presence of catalytic amounts of $Ti(O^nBu)_4$ (*cf.* ESI† for details of synthesis and characterization). By employing different relative amounts of the diol and diester component, polymers **MB34-OMe**, **MB29-OH** and **TB9-OH** with ester or hydroxy end groups, respectively, were generated (*e.g.* **MB29-OH** corresponds to a hydroxy-terminated block copolymer with a molecular weight of M_n(GPC) = 29×10^3 g mol^{-1}). Stabilizers **MB29-OH** and **MB34-OMe** consist of multiple blocks (9 and 11, respectively, number averaged) whereas stabilizer **TB9-OH** is a triblock polymer with a potentially co-crystallizable methylene centre block. Complex **2-py** (Fig. 7) which has proven well suited for polymerizations in THF[11] was employed as a catalyst precursor.

Polymerization in the presence of **MB34-OMe** indeed afforded THF dispersions of colloidally stable submicron particles of high molecular weight polyethylene (Table 3, entries 3–5).

Catalyst stability over time is not compromised by the presence of stabilizer (entries 3 and 4). Even at a stabilizer concentration of less than 10% relative to the amount of polyethylene formed, stable particles were obtained. Increased concentrations of stabilizer result in a reduced particle size, as anticipated (entries 4 and 5). Under otherwise identical conditions, despite a rather high stabilizer concentration the shorter stabilizer **TB9-OH** did not yield colloidally stable particles (entry 6). Also, in control experiments (*cf.* ESI†) in the presence of the C_{48}-dimethyl ester or the PBDD-diol that is the individual free blocks (Fig. 6), respectively, no colloidally stable polyethylene particles were generated. That is, a multiblock nature of the stabilizer is required to achieve colloidal stabilization.

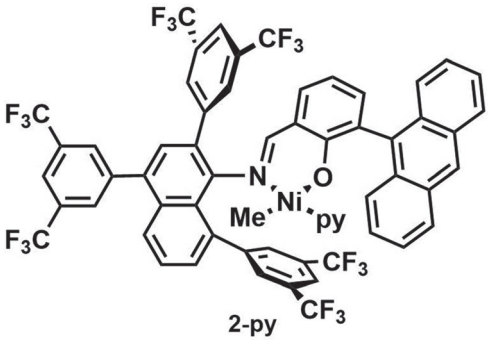

Fig. 7 *N*-Naphtyl-based κ^2-*N*,*O*-salicylaldiminato Ni(II) catalyst precursor used for polymerizations in non-aqueous media.

Compared to polymerization with **MB34-OMe**, in presence of the hydroxy-terminated stabilizer **MB29-OH** polymer yield was decreased (entries 7 and 8). This can be related to catalyst decomposition by protolysis of the growing Ni-polymeryl species by the hydroxyl endgroups.[19] In GPC chromatograms (*cf.* Fig. 9) the formed polyethylene and stabilizer can be differentiated due to their different molecular weights and different CH_3 signature in IR detection. This applies to all types of stabilizers investigated in this work. Note that nominal values of polyethylene molecular weight and molecular weight distribution may be affected to some extent by the cut-off of signals. Notwithstanding, the narrow molecular weight distributions underline the well-behaved nature of polymerization.

Stabilizers with shorter (*i.e.* 16 CH_2 units) linear segments did not result in colloidally stable UHMWPE dispersions. This underlines the necessity of a certain block length of the linear segment and the interplay between linear and THF-soluble segment (*cf.* ESI† for details). For polyethylenes obtained at different stabilizer concentrations under otherwise identical conditions, polyethylene melting points appear to decrease somewhat with increasing stabilizer content.

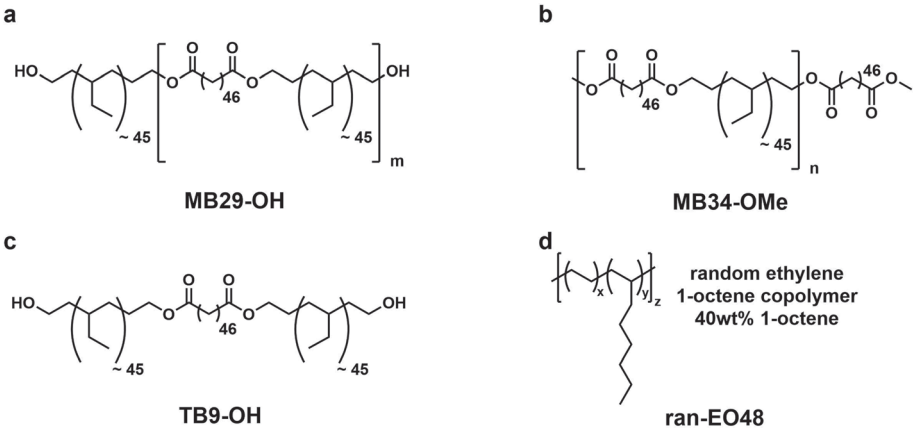

Fig. 6 (a) Precise block length multiblock copolymer with crystallizable linear and branched soluble blocks and OH endgroups. (b) Precise block length multiblock copolymer with crystallizable linear segments and branched soluble blocks and OMe endgroups. (c) Triblock polymer with a central linear and terminal branched blocks. (d) Random ethylene-octene copolymer.

Table 3 Ethylene polymerization experiments in THF with multiblock copolymers as stabilizers

Entry	Stabilizer	$m_{stabilizer}$ [g]	$t_{reaction}$ [°C]	$T_{reaction}$ [min]	Yield [g]	Chains/[Ni]	$d_{particle}$ [a] [μm]	Colloidal stability	T_m [b] [°C]	χ [b] [%]	M_n [c] [$\times 10^6$ g mol^{-1}]	M_w/M_n [c]
1 [d]	None	—	40	30	3.6	0.7	—	—	141 (134)	62 (34)	0.6	1.06
2 [d]	None	—	60	30	16.6	n.d.	—	—	136 (127)	54 (36)	n.d.	n.d.
3	**MB34-OMe**	0.2	40	30	0.93	0.5	1.0	Stable	141 (133)	49 (34)	0.4	1.2
4	**MB34-OMe**	0.2	40	60	2.58	0.5	0.9	Stable	140 (133)	63 (39)	1.0	1.07
5	**MB34-OMe**	1.0	40	60	1.93	0.5	0.6	Stable	134 (130)	36 (22)	0.8	1.1
6	**TB9-OH**	1.0	40	60	1.70	0.5	—	Aggregated	141 (133)	41 (27)	0.7	1.2
7	**MB34-OMe**	1.0	60	30	4.21	0.8	—	Aggregated	129 (124)	48 (32)	1.0	1.2
8	**MB29-OH**	0.2	60	30	2.81	0.6	—	Aggregated	134 (126)	46 (31)	1.0	1.2

Polymerization conditions: 5 μmol of catalyst precursor **2-pyr** (entries 1 and 2 performed with 10 μmol of **2-pyr**), 100 mL THF, 40 bar ethylene. [a] Determined from SEM images. [b] Determined by DSC at a heating/cooling rate of 10 K min^{-1}, data reported from first heating cycles, data from second heating cycles is given in brackets. [c] Determined by gel permeation chromatography in *o*-DCB at 160 °C *via* universal calibration with polystyrene standards. Only the molecular fraction identified as PE *via* IR detection is considered. [d] 10 μmol of catalyst precursor.

Table 4 Polymerization experiments in THF and *n*-heptane with **ran-EO48** as a stabilizer

Entry	$m_{stabilizer}$ [g]	$t_{reaction}$ [min]	Yield [g]	Chains/[Ni]	$d_{particles}$ [a] [μm]	Colloidal stability	T_m [b] [°C]	χ [b] [%]	M_n [c] [$\times 10^6$ g mol^{-1}]	M_w/M_n [c]
1 [d]	—	30	16.6	n.d.	—	Aggregated	136 (127)	54 (36)	n.d.	n.d.
2	0.2	60	9.7	1.5		Aggregated	130 (124)	54 (35)	1.3	1.4
3	0.4	30	4.8	1.0		Aggregated	129 (123)	51 (32)	1.0	1.3
4	0.6	30	2.9	0.4		Aggregated	129 (124)	52 (34)	1.5	1.2
5	0.8	30	6.3	1.0	2.8	Stable	128 (124)	51 (34)	1.3	1.3
6	1.2	30	5.4	0.8	3.2	Stable	130 (124)	43 (28)	1.3	1.3
7	—	30	5.1	0.9	—	Aggregated	139 (132)	63 (40)	1.1	1.1
8	0.4	30	3.1	0.5	—	Aggregated	138 (132)	60 (41)	1.3	1.1
9	0.6	30	4.7	0.8	1.8	Stable	140 (132)	59 (40)	1.2	1.06
10	0.8	30	3.5	0.5	1.7	Stable	140 (134)	55 (36)	1.4	1.1
11	1.2	30	3.6	0.6	1.9	Stable	138 (132)	52 (34)	1.3	1.09
12	1.2	60	7.4	1.2	—	Aggregated	138 (133)	59 (38)	1.3	1.2
13	2.4	60	7.1	1.0	1.6	Stable	137 (132)	53 (32)	1.4	1.2

Polymerization conditions: 5 μmol precatalyst **2-pyr** (entry 1: 10 μmol **2-pyr**), 100 mL solvent (entries 1–6 THF, entries 7–13 heptane), 60 °C, 40 bar ethylene. [a] Determined from SEM images. [b] Determined by DSC at a heating/cooling rate of 10 K min^{-1}, data reported from first heating cycles, data from second heating cycles is given in brackets. [c] Determined by gel permeation chromatography in TCB at 160 °C with refractive index (concentration signal), viscosity and light scattering detection (15° and 90°). Molecular weights were determined using the triple detection method calibrated with narrow polystyrene standards. [d] 10 μmol of catalyst precursor.

This possibly indicates co-crystallization of the formed polyethylene with the linear multiblock copolymer sequences.

In addition to these well-defined multiblock copolymers a commercially available random ethylene/1-octene copolymer was probed as a stabilizer. The choice of composition is a trade-off between sufficiently long linear crystallizable ethylene-based blocks, and solubility provided by the octene-based branches. Based on the above observation of the suitability of C_{46} blocks in the multiblock copolymers, an ethylene-octene copolymer with 40 wt% octene was chosen as a compromise between a relevant content of such long ethylene blocks and a high branch content (*cf.* Fig. S3 in the ESI† for a statistical consideration of block lengths in random copolymers *vs.* comonomer content).

As a reference with regard to particle structures (*vide infra*), polymerizations in *n*-heptane as a typical hydrocarbon medium were also studied. Note that the multiblock copolymer stabilizers are not applicable in *n*-heptane due to their poor solubility in the reaction medium. Polymerization experiments in THF as well as in *n*-heptane with **2-pyr** in the presence of this copolymer ($M_n = 45 \times 10^3$ g mol^{-1}, M_w/M_n 1.7) as a stabilizer yielded colloidally stable UHMWPE particles even at elevated reaction temperatures of 60 °C.

A colloidally stable nature of the formed polyethylene was observed in experiments with stabilizer contents (relative to polymer formed) as low as *ca.* 13 wt% for polymerization in both media. Particle sizes of the obtained UHMWPE dispersions are also in a comparable range.

Particle structures

For both, particles obtained in THF and in heptane, scanning electron microscopy confirms particle sizes on the order of a few μm diameter consisting of randomly ordered lamellae. The lamellae are agglomerated into spherical particles. This is in contrast to the bowtie-shaped morphology found by Rastogi and co-workers[8] (Fig. 8, top left, centre and right). In samples obtained from polymerizations that yielded aggregated polymer, the initial spherical particles aggregate into larger raspberry shaped units. The initial lamella morphology is still

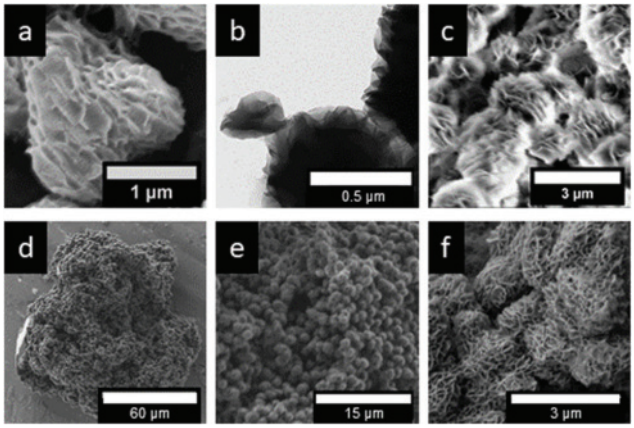

Fig. 8 (a) SEM and (b) TEM image of particles of colloidally stable UHMWPE from THF, and (c) SEM image of particles from heptane. (d–f) SEM micrographs of aggregated particles from THF at increasing magnifications.

evident (Fig. 8, bottom, left to right). To further probe the interaction of the stabilizers with polymer particles, the formed UHMWPE was subjected to soxhlet extraction with THF. GPC traces of the extracted UHMWPE suggest that the stabilizer has been removed virtually completely. This is also confirmed by GPC detected by IR spectroscopy, which is sensitive to branching (Fig. 9). This suggests qualitatively that the stabilizers are physically absorbed to the particle surface, likely forming ordered epitaxial crystalline structures, but not intimately co-crystallized into the UHWMPE lamellae. The ability to remove the stabilizer is also practically advantageous, in view of a recycling of the stabilizers into the polymerization process.

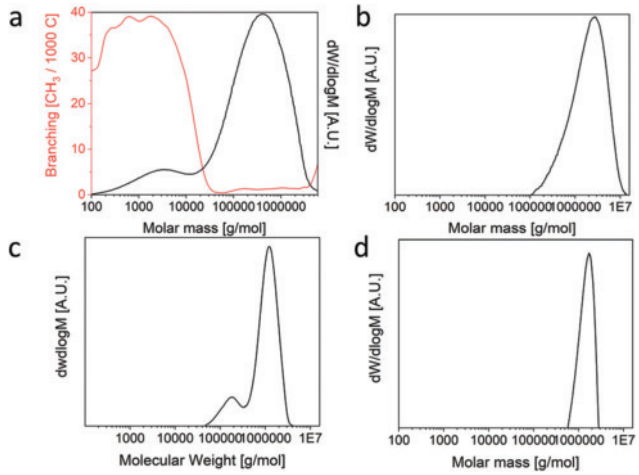

Fig. 9 (a) GPC trace of UHMWPE (Table 4, entry 6) as obtained from polymerization. Branching densities (red) monitored by the IR detector allow for differentiation of the linear (UHMW)PE generated from the branched **ran-EO48** stabilizer employed. (b) GPC trace after soxhlet extraction. The absence of low-molecular weight and highly branched fraction indicates exhaustive removal of the stabilizer. (c) GPC trace of UHMWPE (Table 3, entry 4) as obtained from polymerization. (d) GPC trace after soxhlet extraction. The absence of the low-molecular weight fraction indicates exhaustive removal of the **MB34-OMe** multiblock copolymer stabilizer.

Summary and conclusions

Using common lipophilic catalyst precursors with state-of-the art chelated Ni(II) motifs, UHMWPE can be obtained in the form of (sub)micron aqueous and non-aqueous colloidally stable particle dispersions. In aqueous systems, utilization of a weakly-coordinated reactive catalyst precursor is decisive to enable catalyst activation also at the relatively high local concentration present in the initial catalyst miniemulsion. As expected, low molecular weight ionic surfactants are suited for particle stabilization in aqueous systems while non-aqueous systems require steric stabilizers. Such stabilizers that provide interactions with polyethylene particles by means of linear PE segments as well as soluble branched segments were found to be suitable. Studies of multiblock copolymers with precise block length, obtained from polyesterification of corresponding macromonomers, showed the chain length of the PE-binding linear segments of the stabilizer and the number of such segments per stabilizer molecule have a strong impact on colloidal stabilization. This suggests an epitaxial crystalline interaction of steric stabilizer molecules with the surface of the polyethylene particles. DSC measurements at different heating rates show the polymers obtained from aqueous emulsion polymerization to have a low level of entanglements.

Author contributions

The manuscript was written through contributions of all authors. All authors have given approval to the final version of the manuscript.

Conflicts of interest

The authors declare no conflicts of interests.

Acknowledgements

Financial support by SABIC is gratefully acknowledged. The authors thank Nic Friederichs, Enrico Troisi and Dieter Bilda for fruitful discussions. We thank Marina Krumova for assistance with TEM imaging. Assistance with SEM imaging by Michael Laumann is gratefully acknowledged.

Notes and references

1 D. Jeremic, *Polyethylene, in Ullmann's Encyclopedia of Industrial Chemistry*, Wiley online library, Weinheim, 7th edn, 2000.

2 T. Deplancke, O. Lame, F. Rousset, I. Aguili, R. Seguela and G. Vigier, Diffusion versus Cocrystallization of Very Long Polymer Chains at Interfaces: Experimental Study of Sintering of UHMWPE Nascent Powder, *Macromolecules*, 2014, **47**, 197–207.
3 T. A. Tervoort, J. Visjager and P. Smith, On Abrasive Wear of Polyethylene, *Macromolecules*, 2002, **35**, 8467–8471.
4 S. Rastogi, K. Garkhail, R. Duchateau, G. J. M. Gruter and D. R. Lippits, *Process for the preparation of a shaped part of an ultra high molecular weight polyethylene*, WO2004113057A1, 2004, Dutch Polymer Institute.
5 A. Pandey, Y. Champouret and S. Rastogi, Heterogeneity in the Distribution of Entanglement Density during Polymerization in Disentangled Ultrahigh Molecular Weight Polyethylene, *Macromolecules*, 2011, **44**, 4952–4960.
6 P. J. Lemstra, N. A. J. M. van Aerle and C. W. M. Bastiaansen, Chain-Extended Polyethylene, *Polym. J.*, 1987, **19**, 85–98.
7 S. Rastogi, D. R. Lippits, G. W. H. Höhne, B. Mezari and P. C. M. M. Magusin, The role of the amorphous phase in melting of linear UHMW-PE; implications for chain dynamics, *J. Phys.: Condens. Matter*, 2007, **19**, 205122.
8 S. Ronca, G. Forte, A. Ailianou, J. A. Kornfield and S. Rastogi, Direct Route to Colloidal UHMWPE by Including LLDPE in Solution during Homogeneous Polymerization of Ethylene, *ACS Macro Lett.*, 2012, **1**, 1116–1120.
9 P. Kenyon and S. Mecking, Pentafluorosulfanyl Substituents in Polymerization Catalysis, *J. Am. Chem. Soc.*, 2017, **139**, 13786–13790.
10 S. Mecking and M. Schnitte, Neutral Nickel(II) Catalysts: From Hyperbranched Oligomers to Nanocrystal-Based Materials, *Acc. Chem. Res.*, 2020, **53**, 2738–2752.
11 P. Kenyon, M. Wörner and S. Mecking, Controlled Polymerization in Polar Solvents to Ultrahigh Molecular Weight Polyethylene, *J. Am. Chem. Soc.*, 2018, **140**, 6685–6689.
12 M. Schnitte, J. S. Scholliers, K. Riedmiller and S. Mecking, Remote Perfluoroalkyl Substituents are Key to Living Aqueous Ethylene Polymerization, *Angew. Chem., Int. Ed.*, 2020, **59**, 3258–3263.
13 M. Schnitte, A. Staiger, L. A. Casper and S. Mecking, Uniform shape monodisperse single chain nanocrystals by living aqueous catalytic polymerization, *Nat. Commun.*, 2019, **10**, 2592.
14 J.-C. Daigle, F. P. Lucien, P. B. Zetterlund and J. P. Claverie, Water and Carbon Dioxide: A Unique Solvent for the Catalytic Polymerization of Ethylene in Miniemulsion, *Chem. – Asian J.*, 2017, **12**, 2057–2061.
15 R. Soula, C. Novat, A. Tomov, R. Spitz, J. Claverie, X. Drujon, J. Malinge and T. Saudemont, Catalytic Polymerization of Ethylene in Emulsion, *Macromolecules*, 2001, **34**, 2022–2026.
16 F. M. Bauers and S. Mecking, High Molecular Mass Polyethylene Aqueous Latexes by Catalytic Polymerization, *Angew. Chem., Int. Ed.*, 2001, **40**, 3020–3022.
17 I. Göttker-Schnetmann, B. Korthals and S. Mecking, Water-soluble salicylaldiminato Ni(II)-methyl complexes: enhanced dissociative activation for ethylene polymerization with unprecedented nanoparticle formation, *J. Am. Chem. Soc.*, 2006, **128**, 7708–7709.
18 I. Göttker-Schnetmann and S. Mecking, A Practical Synthesis of [(tmeda)Ni(CH_3)$_2$], Isotopically Labeled [(tmeda)Ni($^{13}CH_3$)$_2$], and Neutral Chelated-Nickel Methyl Complexes, *Organometallics*, 2020, **39**, 3433–3440.
19 A. Godin, I. Göttker-Schnetmann and S. Mecking, Nanocrystal Formation in Aqueous Insertion Polymerization, *Macromolecules*, 2016, **49**, 8825–8837.
20 S. Rastogi, D. R. Lippits, G. W. M. Peters, R. Graf, Y. Yao and H. W. Spiess, Heterogeneity in polymer melts from melting of polymer crystals, *Nat. Mater.*, 2005, **4**, 635–641.
21 D. R. Lippits, *Controlling the melting kinetics of polymers: a route to a new melt state*, Ph.D. Thesis, Eindhoven, 2007.
22 P. Smith, H. D. Chanzy and B. P. Rotzinger, Drawing of virgin ultrahigh molecular weight polyethylene: An alternative route to high strength/high modulus materials, *J. Mater. Sci.*, 1987, **22**, 523–531.
23 T. Witt, M. Häußler, S. Kulpa and S. Mecking, Chain Multiplication of Fatty Acids to Precise Telechelic Polyethylene, *Angew. Chem., Int. Ed.*, 2017, **56**, 7589–7594.
24 P. S. Gopala Krishnan, K. Ayyaswamy and S. K. Nayak, Hydroxy Terminated Polybutadiene: Chemical Modifications and Applications, *J. Macromol. Sci., Part A: Pure Appl.Chem.*, 2013, **50**, 128–138.